

## **Chapter 2**

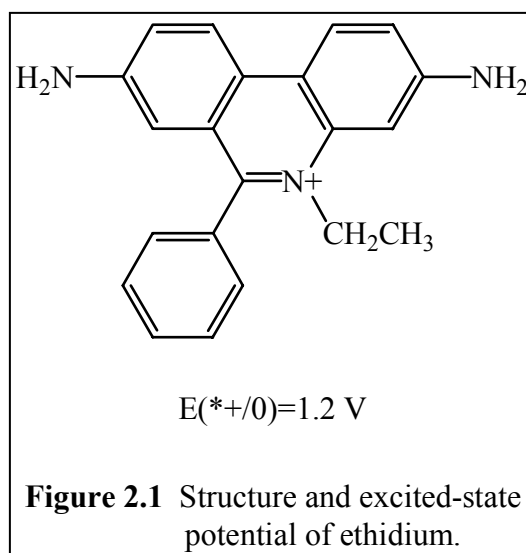
### **Spectroscopy of Ethidium/7-Deazaguanine-Modified DNA Assemblies<sup>‡</sup>**

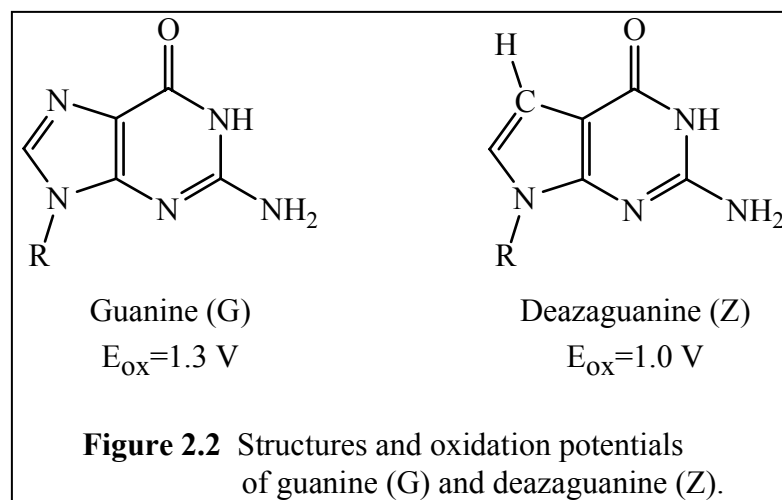
<sup>‡</sup>Femtosecond time-resolved laser experiments performed in collaboration with Professor Ahmed H. Zewail, Dr. Chaozhi Wan, and Dr. Torsten Fiebig in the Laboratory for Molecular Sciences at the California Institute of Technology.

## 2.1 Introduction

Efficient, long-range charge transfer mediated by the DNA base stack has been observed in many different systems.<sup>1-4</sup> Utilizing intercalating reactants which are well coupled to the DNA  $\pi$  stack reveals a shallow distance dependence for charge transfer between donors and acceptors *through* the DNA double helix.<sup>5</sup> To simplify the reaction even further, a modified DNA base (which is an integral structural and electronic component of the  $\pi$  stack) was employed to investigate charge transfer.<sup>6</sup> Kelley and Barton examined the fluorescence quenching of the classical organic intercalator ethidium (Figure 2.1) by the photooxidation of the modified base 7-deazaguanine (Z, Figure 2.2) (*vide infra*).

Ethidium is a useful probe, as it readily intercalates into the minor groove of the DNA double helix, and its excited state ( $n-\pi^*$ ) is fluorescent ( $\lambda_{\text{max}}$  ca. 600 nm).<sup>7</sup> Importantly, excited-state ethidium is capable of oxidizing 7-deazaguanine ( $E(+/0) = 1.0$  V) but not guanine ( $E(+/0) = 1.3$  V).<sup>6,8</sup> This allows us to treat Et/G duplexes, where charge transfer is thermodynamically unfavorable, as references to Et/Z systems in which charge transfer is expected to occur ( $\Delta G = -0.2$  V).

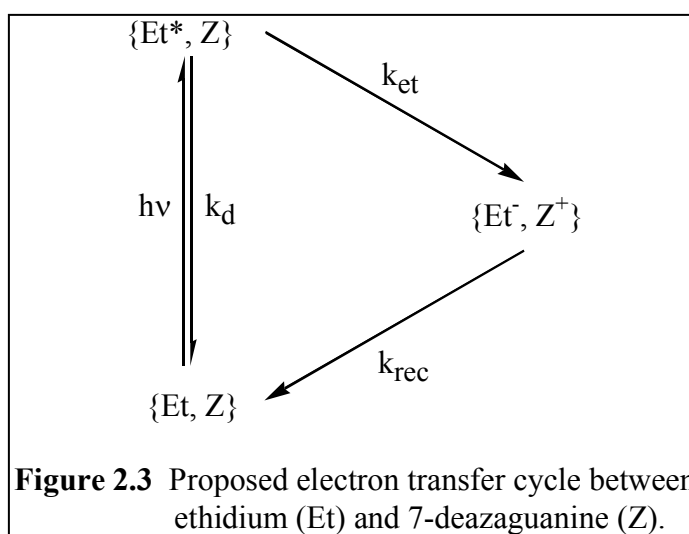




7-Deazaguanine (Z) differs from guanine (G) only in the change of a nitrogen to a C-H unit. The hydrogen bonding, stacking, and structural stability it provides should be very similar to that of the natural base guanine. The one important difference between Z and G is the lower (by 0.3 V) oxidation potential of 7-deazaguanine. The site of 7-deazaguanine incorporation into DNA duplexes is easily controlled via automated oligonucleotide synthesis. Barton and Kelley utilized this to create a series of well-defined duplexes in which the donor/acceptor (Et/Z) distances could be easily determined and varied systematically.<sup>6</sup> Several DNA duplexes were created in which the ethidium was tethered to one end of the DNA duplex. The tethered Et intercalated within the first few base pairs from the end of the duplex and participated in charge transfer with Z according to the scheme outlined below in Figure 2.3.

Extraordinarily efficient charge transfer was observed over a large range of Et/Z separations (10–30 Å). The charge transfer was also quite fast ( $>10^9 \text{ s}^{-1}$ ) and was not able to be resolved using typical time-resolved subnanosecond fluorescence spectroscopy. To obtain this valuable information, measurements need to be taken on a laser system with a much shorter time resolution. This chapter presents femtosecond time-resolved spectroscopic results of charge transfer involving ethidium and 7-deazaguanine, both in DNA duplexes and free in solution. Further structural characterizations of ethidium-

modified duplexes are presented, and the noncovalent interactions of ethidium and 7-deazaguanine in solution are also detailed. These studies clearly demonstrate the importance of structure, stacking, and dynamics on charge transfer through the DNA base stack.



## 2.2 Experimental Section

*Materials.* Reagents for DNA oligonucleotide synthesis were obtained from Glen Research, and nucleotide triphosphates were purchased from Pharmacia. Unless otherwise noted, all other chemicals were purchased from Fluka or Aldrich and used without further purification.

*Instrumentation.* UV-visible spectra were taken on either an HP 8452A spectrophotometer or a Beckman DU 7400 spectrophotometer. Time-resolved fluorescence and transient absorption measurements on the femtosecond timescale were carried out in the facilities in the Laboratory for Molecular Sciences using a Ti:sapphire laser (Spectra-Physics), as has been described.<sup>9</sup> Steady-state emission from 500–800 nm was measured using an ISS K2 spectrofluorometer with  $\lambda_{exc} = 480$  nm. NMR spectra were acquired on a Varian Unity Plus 600 MHz spectrometer.

*Methods. Sample Preparation.* Unless otherwise noted, all experiments were performed in a buffer of 5 mM sodium phosphate (NaPi), 50 mM sodium chloride (NaCl), at pH=7. Ethidium-modified duplexes and 7-deazaguanine containing duplexes were synthesized as previously described.<sup>6,10</sup> All conjugates were purified by reverse phase HPLC (0–35% CH<sub>3</sub>CN over 50 minutes). The ethidium concentration ( $\epsilon_{480} = 5680 \text{ M}^{-1}\text{cm}^{-1}$ ) in the nucleotide studies was 100  $\mu\text{M}$ , and the ethidium-modified duplex concentration in the DNA studies was 10  $\mu\text{M}$ . Duplexes were created by hybridizing the appropriate amounts of complementary single strands based on the extinction coefficients for ethidium-modified sequences ( $\epsilon_{484} = 4000 \text{ M}^{-1}\text{cm}^{-1}$ ) and calculated extinction coefficients for unmodified sequences ( $\epsilon_{260} \text{ (M}^{-1}\text{cm}^{-1})$ ): dC = 7400; dT = 8700; dG = 11,500; dA = 15,400; dZ = 10,500.<sup>6,11,12</sup> Characterization for all oligonucleotides included MALDI-TOF mass spectrometry and UV-visible spectroscopy.

*Time-resolved Spectroscopy.* Time-resolved data were obtained by Dr. Chaozhi Wan and Dr. Torsten Fiebig in the Laboratory for Molecular Sciences at the California Institute of Technology. A Ti:sapphire laser generated femtosecond pulses (80 fs; ca. 800 nm; 2 mJ at 1 kHz). The 2-mJ pulse was split equally to pump two optical parametric amplifiers (OPAs). The signal output from one OPA was then mixed with the residual 800 nm pulse to generate the pump pulse at 480–520 nm. The probe pulse at 570–700 nm was generated by doubling the signal from another OPA. The probe pulse at ca. 400 nm was generated by doubling the 800 nm pulse. Pump energy pulses at the sample were approximately 2  $\mu\text{J}$ , and the probe energy pulses were attenuated with filters to be approximately 0.1  $\mu\text{J}$ . Unless otherwise noted, spectra were obtained at ambient temperature (ca. 21 °C).

*Steady-state Spectroscopy.* Steady-state fluorescence measurements were made at ambient temperature (ca. 21 °C) on an ISS K2 fluorometer. Excitation was at 480 nm, and luminescence intensities were integrated from 500–800 nm and compared to a 10  $\mu\text{M}$  Ru(bpy)<sub>3</sub><sup>2+</sup> in H<sub>2</sub>O standard.

*Melting Temperature Experiments.* Thermal denaturation experiments of DNA duplexes were performed on a Beckman DU 7400 spectrophotometer. Absorbance at 260 nm was monitored every 1 degree from 85 to 15 °C, with a 2 minute equilibration time at each step.

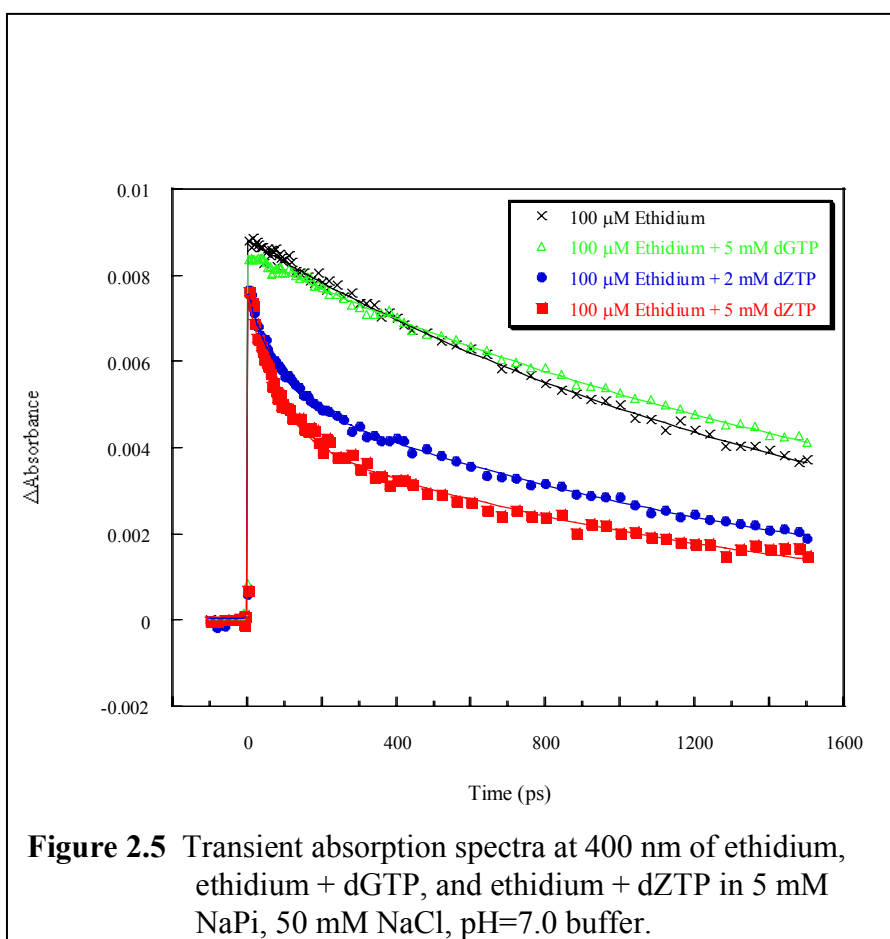
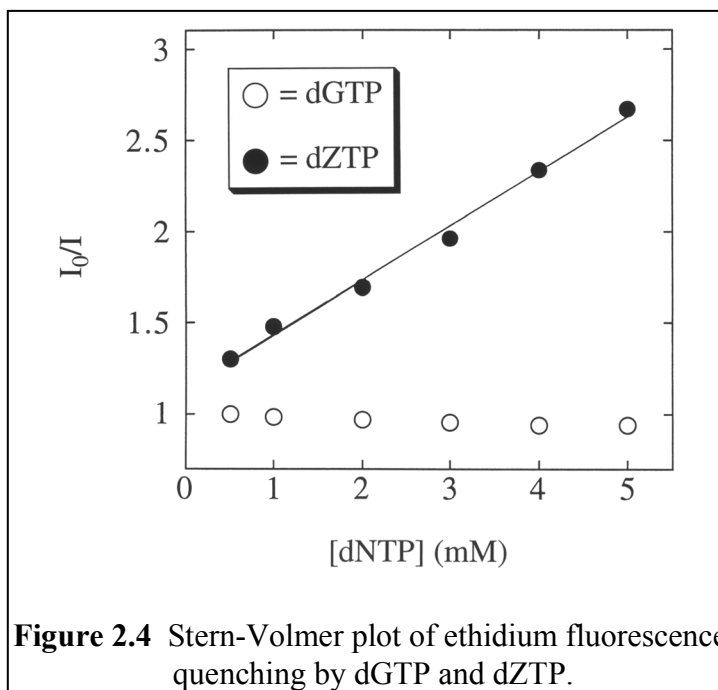
*NMR Experiments.* NMR data acquisition was performed by Dr. Sonya Franklin. Samples for NMR contained 0.1 mM ethidium and 5 mM NaPi, 50 mM NaCl, pH 7.0, in D<sub>2</sub>O plus the appropriate amount of nucleotide triphosphate (dNTP). Spectra were acquired on a Varian Unity Plus 600 MHz spectrometer with a mixing time of 250 ms using Watergate gradient pulse water suppression<sup>13</sup> and analyzed using the program FELIX [Biosym Technologies/Molecular Simulations]. The spectra were referenced to HOD. All spectra were recorded at 25 °C.

## 2.3 Results and Discussion

### 2.3.1 Ethidium-nucleotide interactions and charge transfer

The lowered potential of 7-deazaguanine (1.0 V vs. NHE) compared to guanine (1.3 V vs. NHE) should allow Z to be photooxidized by ethidium. Barton and Kelley verified this by examining the quenching behavior of ethidium by the nucleotide triphosphates dGTP and dZTP.<sup>6</sup> As shown below in Figure 2.4, titrating dGTP into an ethidium-containing solution has little effect of the fluorescence yield. The thermodynamics for charge transfer between Et and dGTP are not favorable, so no luminescence quenching occurs. dZTP, on the other hand, gives rise to efficient luminescence quenching as it is titrated into an ethidium-containing solution. Charge transfer is favorable in this case, and fluorescence quenching occurs with a Stern-Volmer constant of  $K_{SV} = 3 \times 10^2 \text{ M}^{-1}$ .

Time-resolved transient absorption at  $\lambda_{\text{probe}} = 400 \text{ nm}$  of ethidium and the mononucleotides in buffer is shown in Figure 2.5. Data at  $\lambda_{\text{probe}} = 400 \text{ nm}$  and 600 nm are summarized in Table 2.1. The 1–2 ns component of the decay present for all samples



Sample	Probe $\lambda$	$\tau_1$ (ps)	$\tau_2$ (ns)
100 $\mu$ M Et	400 nm	---	1.7 (100%)
100 $\mu$ M Et + 5 mM dGTP	400 nm	---	2.1 (100%)
100 $\mu$ M Et + 2 mM dZTP	400 nm	77 (30%)	1.5 (70%)
100 $\mu$ M Et + 5 mM dZTP	400 nm	75 (43%)	1.3 (57%)
100 $\mu$ M Et	600 nm	---	1.7 (100%)
100 $\mu$ M Et + 5 mM dGTP	600 nm	---	2.2 (100%)
100 $\mu$ M Et + 2 mM dZTP	600 nm	79 (31%)	1.5 (69%)
100 $\mu$ M Et + 5 mM dZTP	600 nm	79 (45%)	1.3 (55%)
<b>Table 2.1</b> Transient absorption lifetimes of Et in 5 mM NaPi, 50 mM NaCl, pH=7.0 buffer in the absence and presence of the nucleotide triphosphates dGTP and dZTP.			

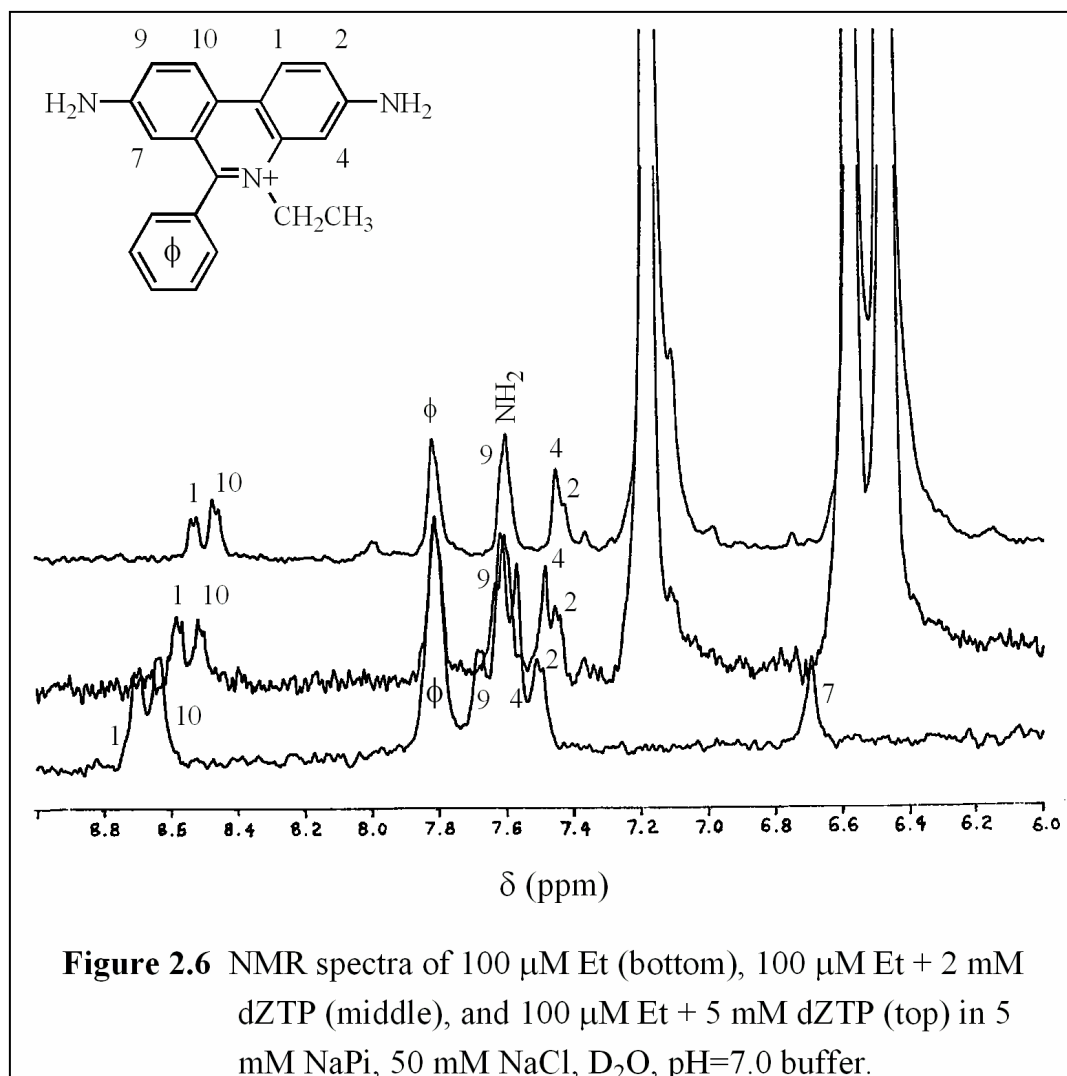
is the typical decay of excited-state ethidium in solution and does not vary with wavelength.<sup>9,14</sup> Adding dGTP to an Et containing solution increases the ethidium lifetime slightly, as dGTP interacts with ethidium in a manner which decreases the chances for a collisional deactivation of the excited state by solvent molecules. Adding dZTP to an ethidium containing solution opens up another pathway (charge transfer between the excited state of ethidium and dZTP) for deactivation to occur. This manifests itself in the ca. 75-ps component that is observed for all Et/dZTP samples.



Interestingly, this rate does not change with increasing dZTP concentration, indicating the reaction is not under diffusion control.

One explanation for the concentration independent rate constant is that the two reactants are pre-associated before the charge transfer occurs. Increasing the dZTP concentration thus creates more of the pre-associated complex which reacts with the same inherent charge transfer rate. Steady-state emission and absorption measurements indicate that Et forms complexes with dGTP and dZTP in aqueous solution, with estimated equilibrium constants of  $300 \text{ M}^{-1}$  for both systems.<sup>9</sup> Theoretical calculations suggested that the electrostatic interaction between the moieties leads to an orientation where the C=O group of the dGTP or dZTP is pointed toward the positively charged ethidium chromophore.<sup>9</sup> These calculations, however, are relevant to the energetics in a vacuum and do not take into account the hydrogen bonding and polar interactions present in aqueous solutions.

Another possible orientation involves the  $\pi$  stacking of the aromatic ethidium and the bases (G or Z) of the nucleotide triphosphates. One way to probe this type of interaction is to look for upfield shifts of peaks in the aromatic region of NMR spectra that are characteristic of  $\pi$ - $\pi$  stacking interactions.<sup>15</sup> Figure 2.6 shows the aromatic region<sup>16</sup> of NMR spectra taken under the conditions of the Et/dZTP time-resolved experiments. The bottom spectrum is that of ethidium in buffer/D<sub>2</sub>O. The middle and top spectra are that of ethidium with 20 and 50 equivalents of dZTP, respectively. Spectra with dGTP under the same conditions show similar chemical shifts. As dZTP (or dGTP) is titrated in, upfield shifts in the aromatic protons (most notably in protons 1 and 10) are observed. No upfield shifts are observed for the phenyl or amine protons, and these are not involved in any direct stacking interactions. The three large peaks that grow in upon dZTP addition are from 7-deazaguanine. Because of their magnitude, it is impossible to determine the extent of the change in chemical shift of these protons.



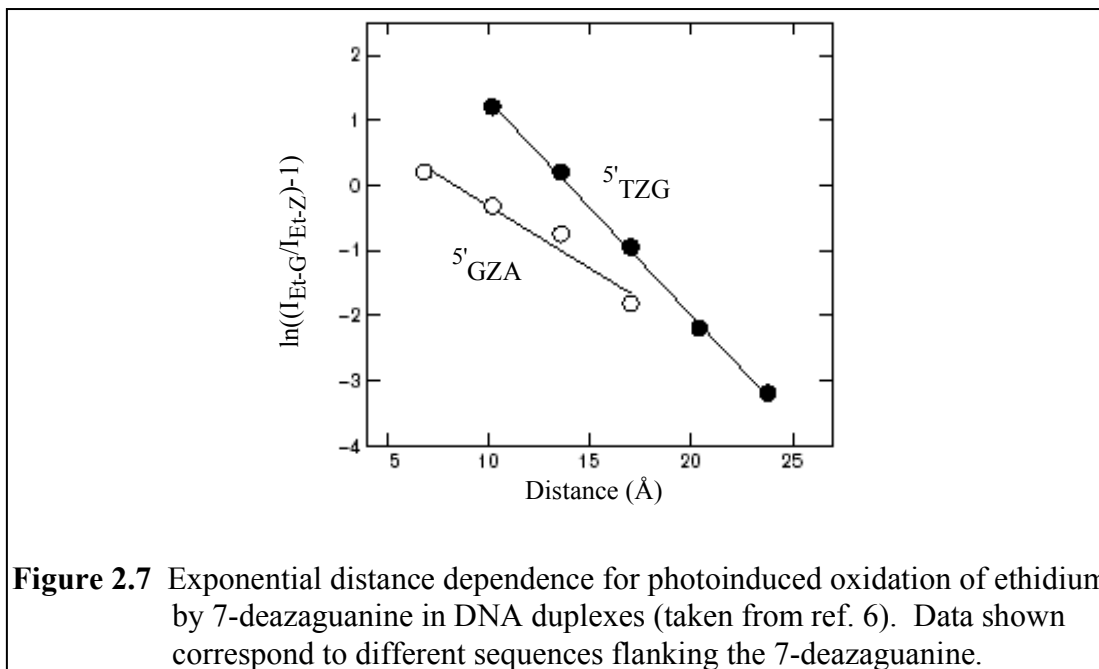
In water, ethidium displays an orientational relaxation time of time of 70 ps.<sup>9</sup> This is remarkably similar to the transient absorption decay times observed in the Et/dZTP samples. It is likely that the fast (ca. 75 ps) component observed in the Et/dZTP samples is an orientational relaxation time that is required within the Et/dZTP before charge transfer can occur. Once this reorientation takes place, charge transfer occurs on a timescale much faster than 75 ps. Any Et/dZTP complexes that do not reorient and free Et in solution will not undergo photoinduced charge transfer. This model is fully consistent with the observed data and underscores the important roles that stacking and dynamics play in mediated charge transfer between aromatic heterocycles.

Other processes occur in the deactivation of the ethidium excited state, but their magnitude is small and much less important to the interpretation of the data described above. A component on the 1-ps timescale is present in all Et, Et/dGTP, and Et/dZTP systems. This is readily ascribed to the relaxation of solvent models surrounding the chromophore dipole as a result of changes in its charge distribution upon excitation.<sup>9,14</sup> Also present on a small scale is a 7-ps component typical of phenyl-group rotation of the phenyl ring on ethidium.<sup>7</sup>

The time-resolved data for ethidium in the presence of nucleotide triphosphates illustrates the complexity often encountered in charge transfer systems. While some of this complexity may be removed by moving to a system in which the reactants are located at fixed distances along the DNA double helix, many challenges still remain. Nevertheless, the lessons learned from the studies with nucleotide triphosphates provide a solid foundation for examining the photoinduced oxidation of 7-deazaguanine at a distance by ethidium through the DNA  $\pi$  stack.

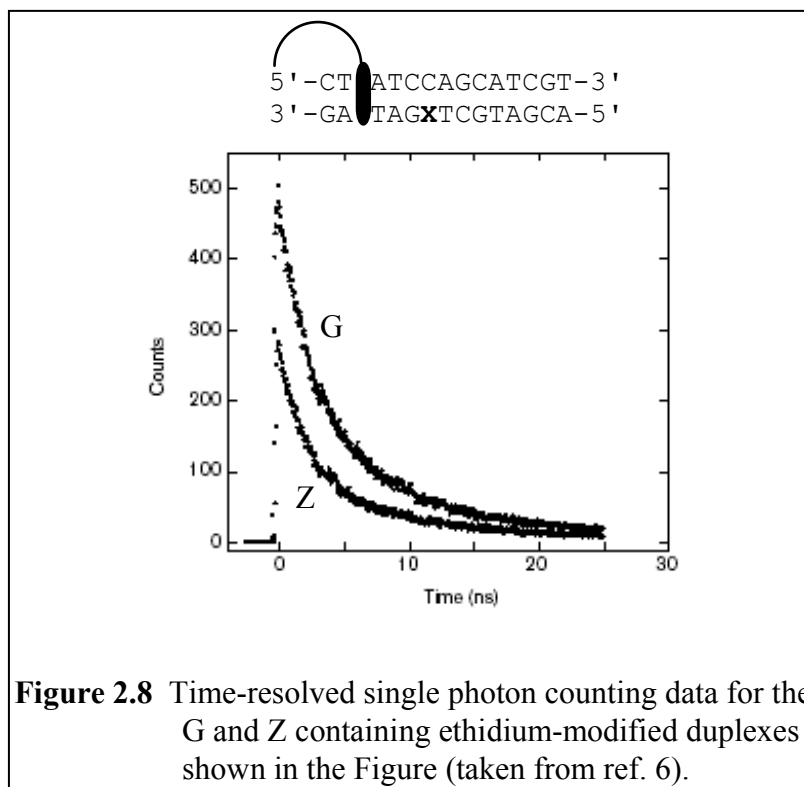
### **2.3.2 Ethidium/7-deazaguanine DNA duplexes and charge transfer**

*Background.* When incorporated into DNA duplexes, 7-deazaguanine is also oxidized by excited-state ethidium. Since the reaction of the excited state of ethidium with the natural DNA bases is not thermodynamically favorable, charge transfer between Z and photoexcited Et can be evaluated without the complications caused by competing reactions. Further, because duplexes containing Z differ from those containing G by only one atom, emission quenching effects are easily attributed to a photoinduced redox process. The discovery of chemistry to reliably attach intercalators to the end of a DNA duplex<sup>17</sup> along with standard automated DNA synthesis led Kelley and Barton to create and characterize a series of duplexes in which ethidium was anchored to the end of the DNA and the 7-deazaguanine was systematically moved further away along the helix.<sup>6</sup> The fluorescence quenching yields in the series of duplexes exhibited a shallow distance



dependence (Figure 2.7) similar to that reported for long-range charge transfer between intercalators.<sup>10</sup> Interestingly, the distance dependence of the Et/Z reaction was sensitive to the flanking sequence of the 7-deazaguanine. A 5'-TZG-3' site showed a steeper quenching distance dependence than a 5'-GZA-3' site ( $0.33 \text{ Å}^{-1}$  vs.  $0.20 \text{ Å}^{-1}$ ). The latter site has two purines flanking the Z reactant; whereas, the former only has one. The additional purine could result in more favorable stacking of the reactant within the helix,<sup>18</sup> which could lead to enhanced donor-acceptor (or donor-bridge/acceptor-bridge) interactions that give rise to a more shallow distance dependence of photooxidative fluorescence quenching.

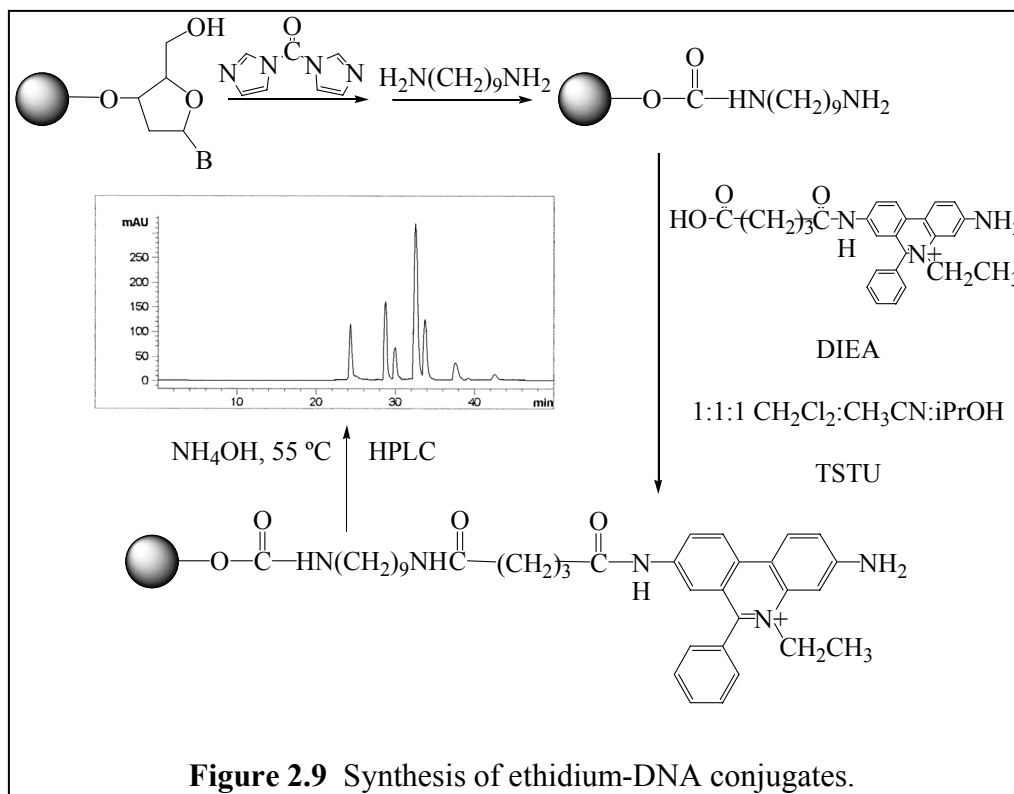
Kelley and Barton also investigated the kinetics of the photoinduced oxidation of Z by Et in DNA using time-correlated single photon counting (TCSPC). In all the Et/Z duplexes studied, ca. 200-ps resolution was not enough to observe dynamic Et fluorescence quenching (see example in Figure 2.8). All of the fluorescence quenching manifests itself as a decrease in initial intensity rather than a decrease in the ethidium excited state lifetime. The observed decays simply correspond to the fluorescence of Et/Z-modified duplexes in which a charge transfer reaction has not taken place.



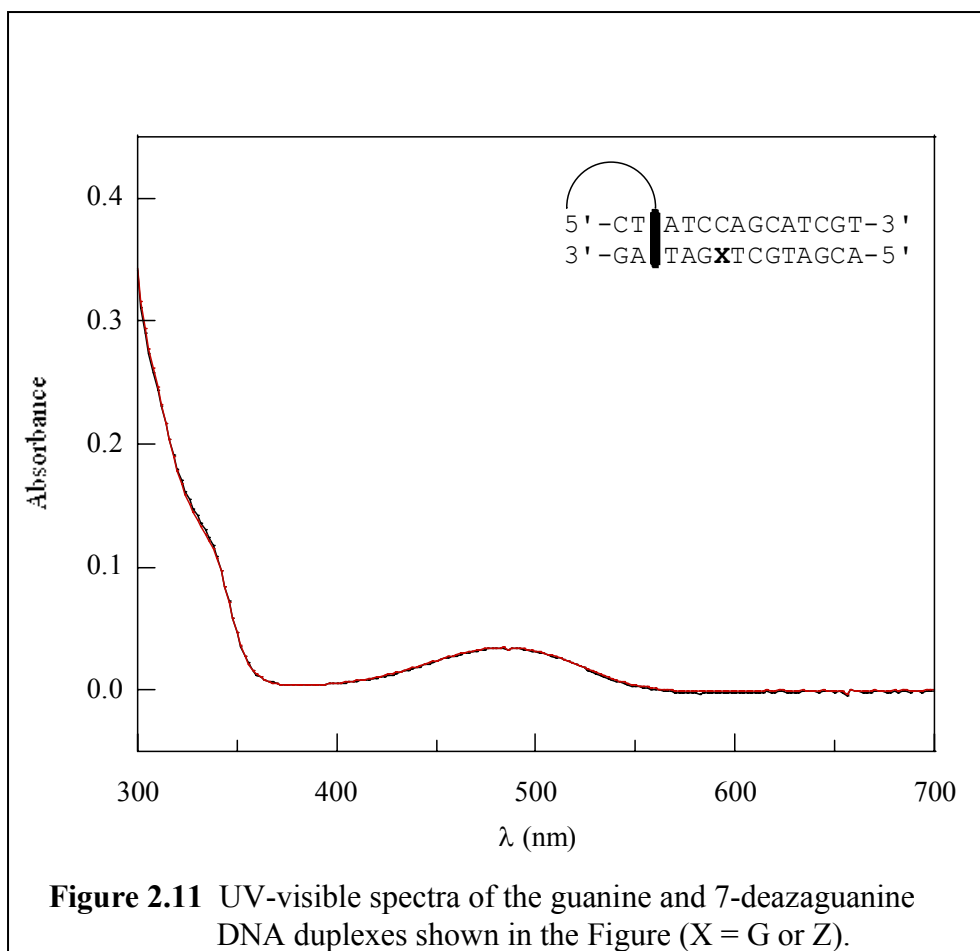
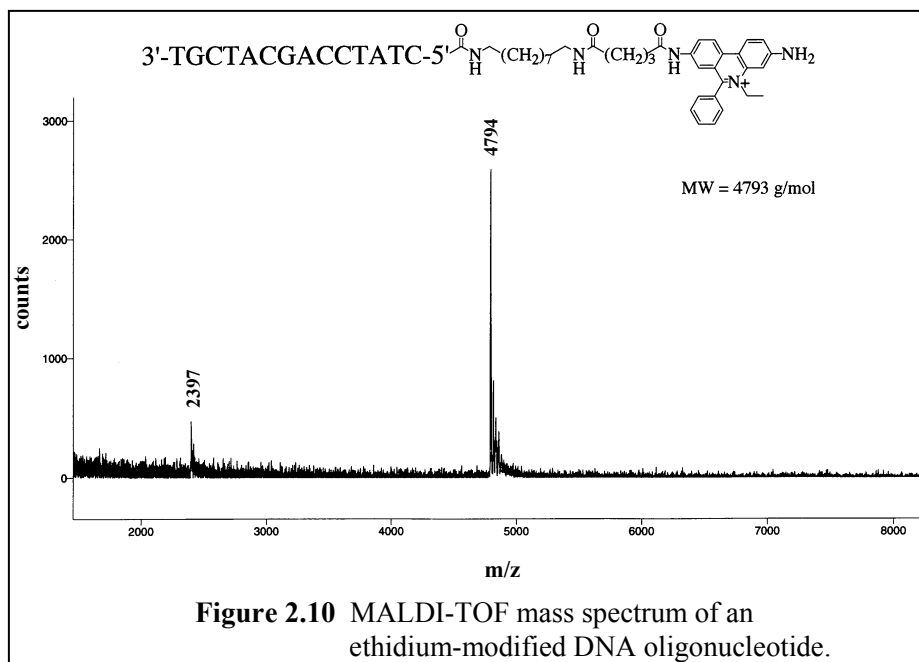
In order to observe charge transfer dynamics between Z and photoexcited Et in DNA, it is necessary to take measurements on a laser system with much shorter time resolution (preferably subpicosecond). The Laboratory for Molecular Sciences at the California Institute of Technology offers such equipment, so we set about synthesizing and characterizing a series of Et/G and Et/Z DNA duplexes to study spectroscopically. Our chosen sequences (Table 2.2, *vide infra*) are a subset of those employed by Kelley and Barton in their previous experiments.<sup>6</sup>


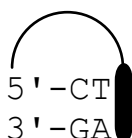
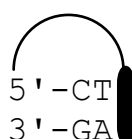
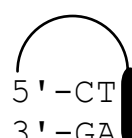

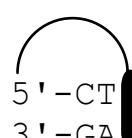
*Et/G and Et/Z conjugates.* The synthesis of ethidium-containing oligonucleotides was performed as outlined previously<sup>6,10,17</sup> and summarized in Figure 2.9. The desired single strand sequence was synthesized on an automated DNA synthesizer and the trityl protecting group removed to leave a 5'-OH on the terminal nucleotide on the controlled pore glass resin (CPG). This was reacted with carbonyl diimidazole followed by a diaminoalkane to form an amine terminated oligonucleotide (still attached to the CPG). Next, a carboxylic acid derivative was coupled to the amine to create an Et-DNA

conjugate, which is still attached to the CPG. This was cleaved from the resin and deprotected in aqueous ammonia and purified via HPLC to give the desired single strand Et-DNA conjugate. MALDI-TOF mass spectrometry (example in Figure 2.10) was used to verify purity.



Ethidium containing strands and G or Z containing strands were then quantitated via UV-visible spectroscopy, and the appropriate amounts were annealed to create Et/G- or Et/Z-modified duplexes. Figure 2.12 shows the UV-visible spectra of similar Et/G and Et/Z duplexes used in the spectroscopy studies. Readily apparent are the  $n\text{-}\pi^*$  absorption near 480 nm typical of ethidium chromophores and the tail of the 260 nm  $\pi\text{-}\pi^*$  band prevalent in DNA.<sup>19</sup> Importantly, the spectra are identical, indicating that substitution of guanine with 7-deazaguanine has no dramatic structural effect on the spectral properties of the photooxidant or its interactions with the DNA base stack. The duplex melting temperatures and fluorescence polarization measurements (Table 2.2) support that notion.

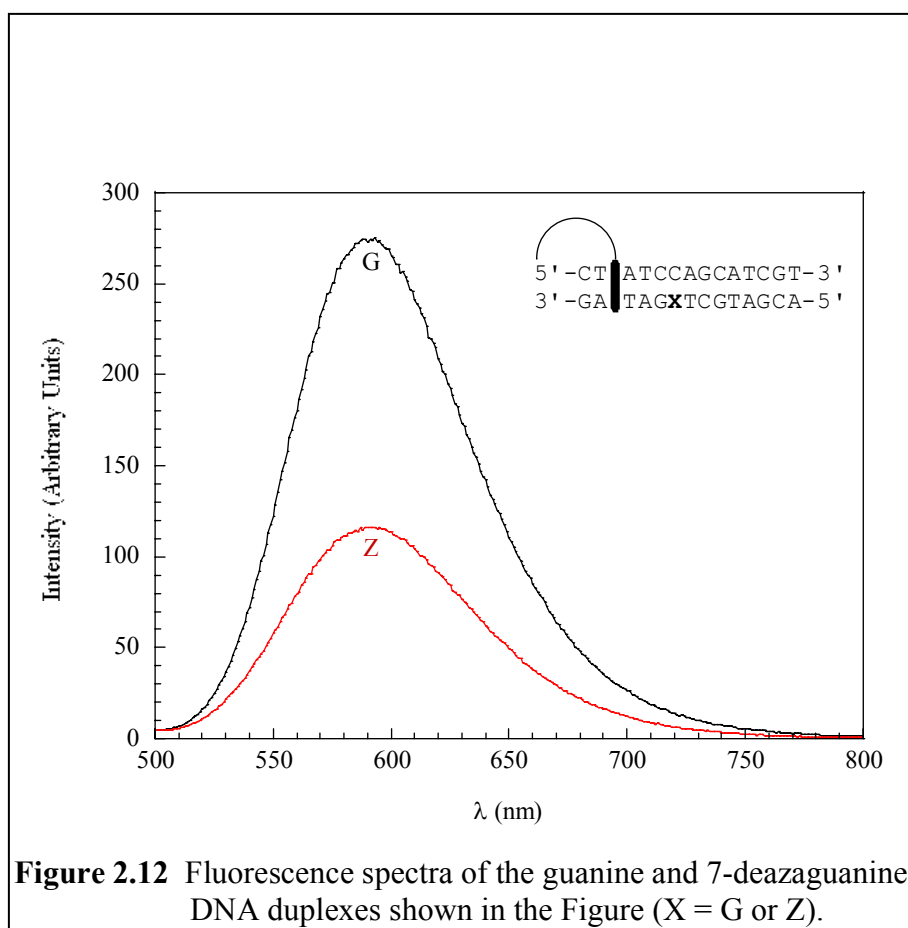


Duplex	$\phi_{\text{REL}}$	Fq	T <sub>m</sub> (°C)	Pol.
 5' -CTTACCAGACATCGT-3' 3' -GATTGGTCTGTAGCA-5'	0.72	---	56	0.243 (1)
 5' -CTTACCAGACATCGT-3' 3' -GATTGTZTCTGTAGCA-5'	0.22	0.70 (5)	55	0.220 (3)
 5' -CTTATCCAGCATCGT-3' 3' -GATTAGGTCGTAGCA-5'	0.80	---	55	0.235 (1)
 5' -CTTATCCAGCATCGT-3' 3' -GATTAGZTCGTAGCA-5'	0.36	0.56 (4)	56	0.227 (2)
 5' -CTTAATCCAGCTCGT-3' 3' -GATTAGGTCGAGCA-5'	0.74	---	56	0.237 (2)
 5' -CTTAATCCAGCTCGT-3' 3' -GATTAGZTCGAGCA-5'	0.54	0.28 (2)	56	0.225 (2)

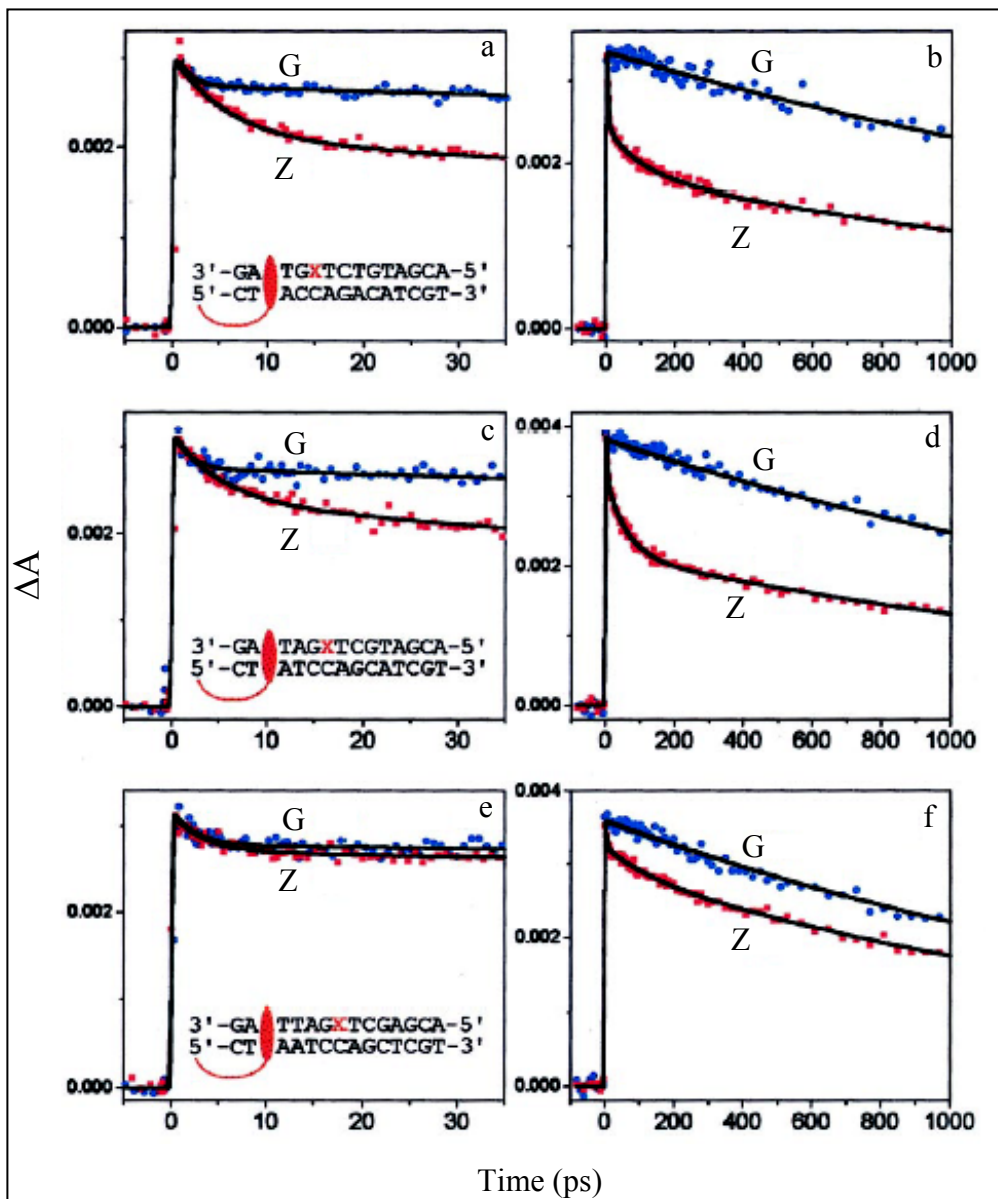
**Table 2.2** Steady-state emission (500–800 nm, relative to 10  $\mu\text{M}$  Ru(bpy)<sub>3</sub><sup>2+</sup>), quenching, melting temperature, and polarization data for 10  $\mu\text{M}$  Et/G and Et/Z DNA duplexes in 5 mM NaPi, 50 mM NaCl, pH=7.





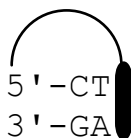

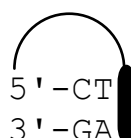

Figure 2.12 shows fluorescence spectra for select G- and Z-modified, ethidium-containing duplexes. Luminescence quenching in the 7-deazaguanine containing duplex is readily apparent. The quantum yields and quenching values for the series of duplexes employed in this study are summarized in Table 2.2. The distance dependence is shallow, and the quenching reaction is quite remarkable considering it was initiated by changing only one atom in an entire DNA duplex.



*Time-resolved Experiments.* Steady-state quenching was easily demonstrated, but what are the dynamics and mechanism of this quenching process? Figure 2.13 illustrates the transient absorption spectra on the picosecond timescale of Et/G- and Et/Z-modified duplexes over a series of donor-acceptor distances. The key data parameters derived from these spectra are summarized in Table 2.3.



**Figure 2.13** Transient absorption of ethidium-modified G and Z containing duplexes (probed at 400 nm after excitation at 500 nm).

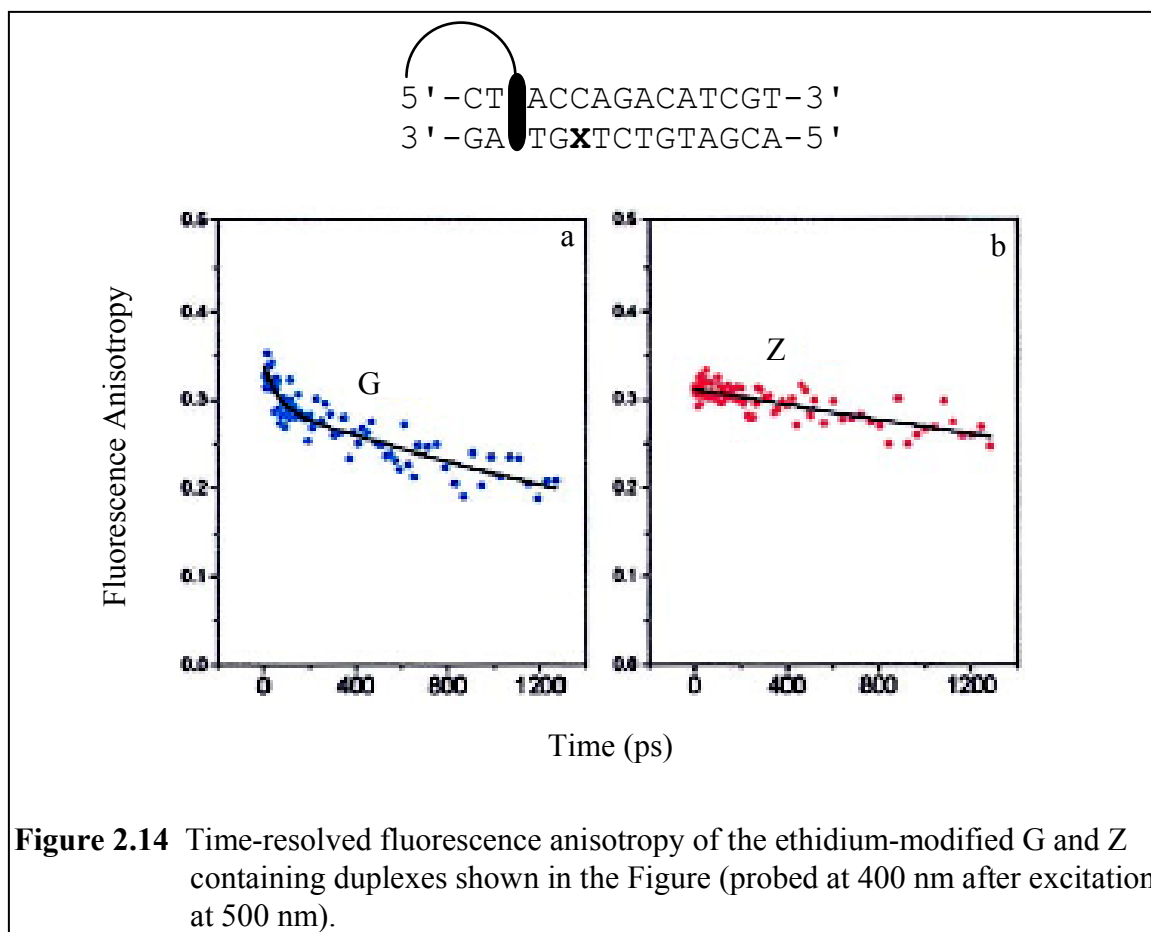
Duplex	$\tau_1$ (ps)	$\tau_2$ (ps)	$\tau_3$ (ns)
 5'-CT[loop]ACCAGACATCGT-3' 3'-GATG <b>G</b> TCTGTAGCA-5'	1.5±0.2 (14%)	---	2.4±0.2 (86%)
 5'-CT[loop]ACCAGACATCGT-3' 3'-GATG <b>Z</b> TCTGTAGCA-5'	5.9±0.6 (34%)	75±10 (23%)	2.1±0.2 (43%)
 5'-CT[loop]ATCCAGCATCGT-3' 3'-GATAG <b>G</b> TCGTAGCA-5'	1.5±0.4 (17%)	---	2.2±0.2 (83%)
 5'-CT[loop]ATCCAGCATCGT-3' 3'-GATAG <b>Z</b> TCGTAGCA-5'	5.1±0.7 (24%)	75±10 (22%)	2.1±0.2 (54%)
 5'-CT[loop]AATCCAGCTCGT-3' 3'-GATTAG <b>G</b> TCGAGCA-5'	2.4±0.5 (12%)	---	2.2±0.2 (88%)
 5'-CT[loop]AATCCAGCTCGT-3' 3'-GATTAG <b>Z</b> TCGAGCA-5'	4.3±0.9 (14%)	103±54 (9%)	2.2±0.2 (77%)

**Table 2.3** Transient absorption lifetimes of Et/G and Et/Z duplexes at 400 nm in 5 mM NaPi, 50 mM NaCl, pH=7 buffer.

All Et/G and Et/Z duplexes display a ca. 2 ns component typical of ethidium excited state decay when tethered and intercalated into DNA. Previous experiments have shown that the nanosecond emission of ethidium tethered to DNA is actually biexponential, but the limits of the instrumentation prevent the longer component (ca. 7 ns) from being observed in these studies.<sup>6,10</sup> Similar to ethidium/nucleotide results, a 1.5-ps decay is observed in all cases that corresponds to solvent reorientation upon excitation of the chromophore. A 20-ps component is also present in negligible amounts, and this is the result of restricted phenyl ring relaxation of the intercalated ethidium.<sup>7</sup>

Replacement of guanine with 7-deazaguanine in ethidium containing duplexes leads to the appearance of short lifetimes on the order of 5 ps and 75 ps. These short components do not change substantially in value but decrease in intensity with increasing donor-acceptor distance. This is inconsistent with a one-step, superexchange model for electron transfer<sup>20</sup> and indicative of more complex interactions between the donor, acceptor, and intervening charge transfer medium. The question then arises as to what physical processes these lifetimes correspond. Theoretical studies<sup>9</sup> have estimated the rate of hole injection from excited-state ethidium into the DNA  $\pi$  stack at 2–4 ps, so assignment of the 5-ps component to this process is not unreasonable. The 75-ps component is similar to the decay observed in the ethidium/nucleotide triphosphate experiments, so we postulated that some sort of dynamical reorientation of ethidium *within* the duplex was giving rise to this decay.

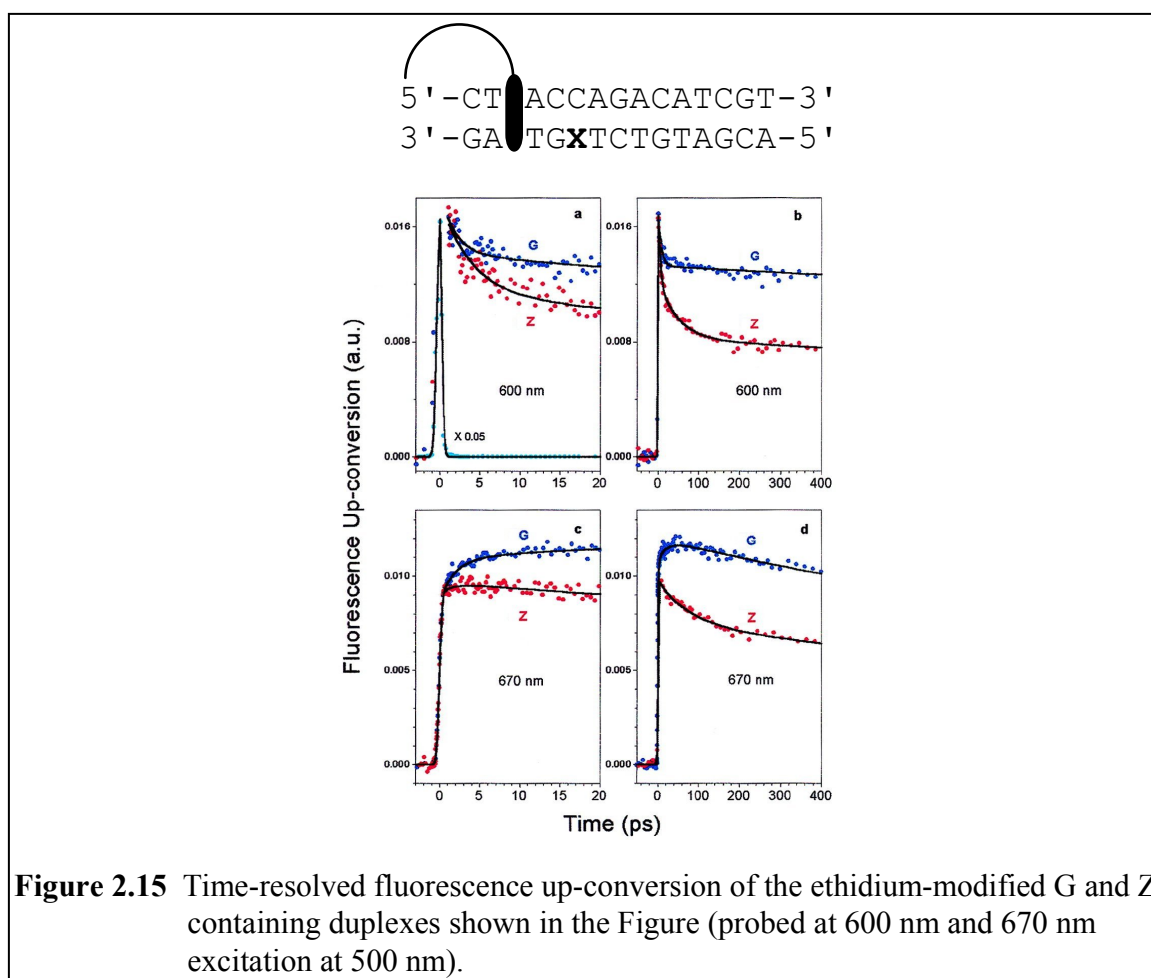
To test this hypothesis the fluorescence anisotropy of G and Z containing Et-modified duplexes was examined (Figure 2.14). The ca. 100-ps component in the anisotropy indicates there is indeed a correlation of the charge transfer process with the reorientation of tethered ethidium within DNA. The reason for the absence of the ca. 100 ps anisotropy in the Et/Z containing duplex in Figure 2.14 is that the faster rotating molecules are immediately drained away by the ET process once they reorient into a favorable geometry for charge transfer.



**Figure 2.14** Time-resolved fluorescence anisotropy of the ethidium-modified G and Z containing duplexes shown in the Figure (probed at 400 nm after excitation at 500 nm).

So in the Et/Z DNA duplexes there are two populations of geometries giving rise to DNA-mediated charge transfer. The first family (5-ps decay) has conformations being initially favorable for charge transfer to occur, while the second (75-ps decay) has conformations being initially unfavorable for charge transfer but being able to reorient to a favorable conformation within the photooxidant's excited-state lifetime. The true number of orientational distributions is more complex, but the charge transfer emphasizes these two groups. We conclude that the 5-ps decay reflects charge transfer dynamics in duplexes where ethidium is “perfectly” stacked and ready for reaction; whereas, the 75-ps component is caused by the fraction of ethidium chromophores that have to reorient within the helix before charge transfer can occur.

To ensure that the decays we were observing arose from the initial excited state of the ethidium population, we performed fluorescence up-conversion measurements. Figure 2.15 shows the fluorescence decays of an Et/G and an Et/Z duplex at 600 nm and 670 nm. Similar to the transient absorption experiments, significant differences between the Et/G and Et/Z samples were recorded. Figures 2.15a and 2.15b ( $\lambda_{\text{obs}} = 600 \text{ nm}$ ) illustrate those differences quite clearly. For Et/G and Et/Z duplexes, there is a 1.5-ps component corresponding to solvation of the excited state. In the Et/Z duplex, 5-ps and 75-ps components are also present, in agreement with the transient absorption results.



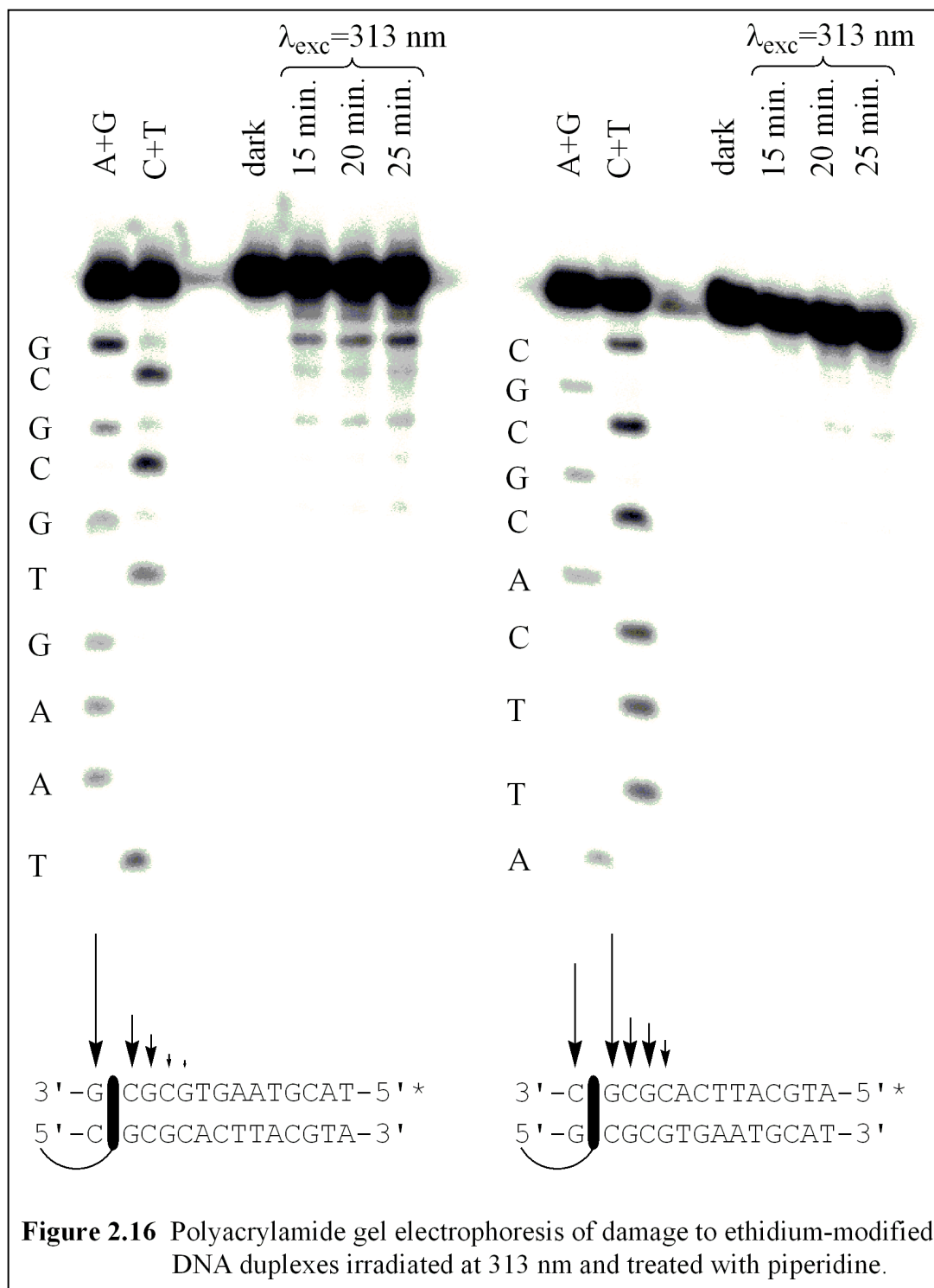
**Figure 2.15** Time-resolved fluorescence up-conversion of the ethidium-modified G and Z containing duplexes shown in the Figure (probed at 600 nm and 670 nm excitation at 500 nm).

Figures 2.15c and 2.15d illustrate the fluorescence up-conversion traces at 670 nm. In these instances the short component is a signal rise instead of a decay. Present in the 670 nm signal rise is a 1.5-ps component and a small percentage (10–20%) of a 20-ps

component. This type of behavior at long (670 nm) vs. short (600 nm) wavelengths reflects a spectral shift caused by solvation dynamics and/or structural relaxation processes, consistent with our assignment of the 1.5-ps component as a solvation process and the 20-ps component as rotation of the phenyl ring on ethidium. These time-resolved fluorescence up-conversion data perfectly complement the transient absorption experiments and make us confident in our assignments of the specific ethidium excited state decay rates.

*Control Experiments.* Can any mechanism other than charge transfer account for the quenching behavior observed in Et/Z DNA duplexes? The one-atom change in going from G to Z makes this unlikely. There is no spectral overlap between the emission of Et and the absorption of Z, so energy transfer may be ruled out. The melting temperature and steady-state polarization data for the duplexes indicated the DNA structure is stable and not perturbed in any significant way.

Others have suggested that the tethered ethidium is in direct contact with the deazaguanine, and that this is why charge transfer occurs. This hypothesis is easily discarded with several observations: (1) The excited state lifetime of non-intercalated, tethered ethidium is never observed in the time-resolved spectroscopy experiments; (2) In order for ethidium to contact the deazaguanine, the structure of the DNA would have to be distorted from standard B-form, a process which is ruled out by the duplex melting temperature and polarization data; (3) Irradiation of ethidium-modified duplexes at 313 nm leads to crosslinking and strand breakage at the site of intercalation.<sup>21,22</sup> This reaction was performed and visualized via polyacrylamide electrophoresis (Figure 2.16), and it was found that over 85% of the tethered ethidium was bound within the first three base pairs of the duplex. As can be seen in Figure 2.16, binding of the intercalator is not fixed at one given site but spread over a few base pairs. Importantly, however, the intercalator is not binding near the 7-deazaguanine, and the observed charge transfer behavior is thus mediated by the DNA  $\pi$  stack.











Further evidence that the DNA base stack is integral charge for efficient charge transfer was provided by introducing a mismatch between the donor and acceptor. CA mismatches, which significantly perturb the DNA  $\pi$  stack relative to a normal TA base pair,<sup>23,24</sup> were incorporated into DNA duplexes between the tethered ethidium intercalator and G or Z. Table 2.4 illustrates the specific sequences and luminescence data for the normal and mismatch containing DNA duplexes. When the normal Watson-Crick DNA base pair (TA) intervenes the donor and acceptor, charge transfer gives rise to a luminescence quenching yield of 56%.

Quenching yields for the duplexes with an intervening CA mismatch are dependent upon which strand contains the cytosine of the CA mismatch. When the C is on the same strand as the 7-deazaguanine, the luminescence quenching yield is reduced to 37%. The less efficient quenching is attributable to a disruption in the DNA base stack between the donor and acceptor. However, when the A of the CA mismatch is on the same strand as the 7-deazaguanine, the luminescence quenching yield is nearly the same (52%) as for the duplex with the normal Watson-Crick base pair. This arises because the adenine remains well stacked within the DNA duplex, while the cytosine on the opposite strand is poorly stacked. The adenine maintains the  $\pi$  stack along the Z containing strand, providing good electronic coupling between donor and acceptor. Thus, charge transfer quenching efficiency is not greatly reduced relative to the normal Watson-Crick paired DNA duplex.

The data from mismatch-containing DNA duplexes demonstrate the importance of base stacking and further underscore the sensitive nature of charge transfer through the DNA double helix. The results shown here agree with other studies on charge transfer through mismatch-containing DNA<sup>10,25,26</sup> and reaffirm that charge transfer in DNA is indeed mediated by the base stack.

Duplex	$\phi_{\text{REL}}$	Fq
 5' -CTATCCAGCATCGT-3' 3' -GATAGGTCGTAGCA-5'	0.80	---
 5' -CTATCCAGCATCGT-3' 3' -GATAGZTCGTAGCA-5'	0.36	0.56
 5' -CTACCCAGCATCGT-3' 3' -GATAGGTCGTAGCA-5'	0.83	---
 5' -CTACCCAGCATCGT-3' 3' -GATAGZTCGTAGCA-5'	0.40	0.52
 5' -CTAACCAGCATCGT-3' 3' -GATCGGTCGTAGCA-5'	0.85	---
 5' -CTAACCAGCATCGT-3' 3' -GATCGZTCGTAGCA-5'	0.54	0.37
<b>Table 2.4</b> Steady-state emission (500–800 nm, relative to 10 $\mu\text{M}$ Ru(bpy) <sub>3</sub> <sup>2+</sup> ) quenching data for 10 $\mu\text{M}$ Et/G and Et/Z mismatch-containing DNA duplexes in 5 mM NaPi, 50 mM NaCl, pH=7 buffer.		

## 2.4 Conclusions

These results detail the mechanism of photoinduced charge transfer in solution and in DNA between an ethidium intercalator and the modified base 7-deazaguanine. The charge transfer quenching of ethidium luminescence by 7-deazaguanine through DNA exhibits a shallow distance dependence. Notably, the apparent rate of charge transfer does not change with increasing donor-acceptor separation. Only the yield of the reaction decreases, indicating decreased stacking (and coupling) within the DNA bridge as the number of bases between donor and acceptor increases. This unique type of quenching behavior must be considered in examining DNA-mediated transfer in a wide variety of systems. These reactions demonstrate the important role stacking and orientational dynamics play in charge transfer and underscore the efficacy with which the DNA  $\pi$  stack is able to mediate charge.

## 2.5 References

1. Holmlin, R. E.; Dandliker, J. K.; Barton, J. K. *Angew. Chem. Int. Ed. Engl.* **1997**, *36*, 2715.
2. Schuster, G. B. *Acc. Chem. Res.* **2000**, *33*, 253.
3. Lewis, F. D.; Letsinger, R. L.; Wasielewski, M. R. *Acc. Chem. Res.* **2001**, *34*, 159.
4. Giese, B. *Acc. Chem. Res.* **2000**, *33*, 631.
5. Treadway, C. R.; Hill, M. G.; Barton, J. K. *Chem. Phys.* **2002**, *281*, 409.
6. Kelley, S. O.; Barton, J. K. *Chem. Biol.* **1998**, *5*, 413.
7. Sommer, J. H.; Nordlund, T. M.; McGuire, M.; McLendon, G. *J. Phys. Chem.* **1986**, *90*, 5173.
8. Steenken, S.; Jovanovic, S. V. *J. Am. Chem. Soc.* **1997**, *119*, 617.
9. Fiebig, T.; Wan, C.; Kelley, S. O.; Barton, J. K.; Zewail, A. H. *Proc. Natl. Acad. Sci. U.S.A.* **1999**, *96*, 1187.
10. Kelley, S. O.; Holmlin, R. E.; Stemp, E. D. A.; Barton, J. K. *J. Am. Chem. Soc.* **1997**, *119*, 9861.
11. Cantor, C. R.; Warshaw, M. M.; Shapiro, H. *Biopolymers* **1970**, *9*, 1059.
12. Warshaw, M. M.; Tinoco, I. *J. Mol. Bio.* **1966**, *1*, 29.
13. Piotto, M.; Saudek, V.; Sklenar, V. *J. Biomol. NMR* **1992**, *2*, 661.
14. Jiminez, R.; Fleming, G. R.; Kumar, P. V.; Maroncelli, M. *Nature* **1994**, *369*, 471.
15. Abraham, R. J.; Fisher, J.; Loftus, P. *Introduction to NMR Spectroscopy*; New York: Wiley, 1988.
16. Laugaa, P.; Delbarre, A.; Le Pecq, J.-B.; Roques, B. P. *Eur. J. Biochem.* **1983**, *134*, 163.
17. Holmlin, R. E.; Dandliker, P. J.; Barton, J. K. *Bioconj. Chem.* **1999**, *10*, 1122.
18. Petersheim, M.; Turner, D. H. *Biochemistry* **1983**, *22*, 256.
19. Saenger, W. *Principles of Nucleic Acid Structure*; New York: Springer-Verlag, 1984.

20. Marcus, R. A.; Sutin, N. *Biochim. Biophys. Acta* **1985**, *811*, 265.
21. Deniss, I. S.; Morgan, A. R. *Nucl. Acids. Res.* **1975**, *3*, 315.
22. Hall, D. B.; Kelley, S. O.; Barton, J. K. *Biochemistry* **1998**, *37*, 15933.
23. Patel, D. J.; Kozlowski, S. A.; Ikuta, S.; Itakura, K. *FASEB* **1984**, *11*, 2664.
24. Brown, T.; Hunter, W. N.; Kneale, G.; Kennard, O. *Proc. Natl. Acad. Sci. U.S.A.* **1986**, *83*, 2402.
25. Kelley, S. O.; Jackson, N. M.; Hill, M. G.; Barton, J. K. *Angew. Chem. Int. Ed. Engl.* **1999**, *38*, 941.
26. Kelley, S. O.; Boon, E. M.; Barton, J. K.; Jackson, N. M.; Hill, M. G. *Nucl. Acids. Res.* **1999**, *27*, 4830.